Organic & Biomolecular Chemistry

Cite this: *Org. Biomol. Chem.*, 2012, **10**, 6850

www.rsc.org/obc

PAPER

Inter- and intrastrand DNA crosslinks by 2-fluoro-substituted pyrrolobenzodiazepine dimers: stability, stereochemistry and drug orientation†

Jenny Seifert,[a] Soheil Pezeshki,[a] Ahmed Kamal[b] and Klaus Weisz*[a]

Received 1st April 2012, Accepted 11th July 2012
DOI: 10.1039/c2ob25654a

A 2-fluoro-substituted pyrrolo[2,1-*c*][1,4]benzodiazepine (PBD) dimer with a 1,4-di-*n*-propyl piperazine linker was studied with respect to its binding and crosslinking capability towards double-helical DNA targets. Duplex thermal stabilizations upon drug binding as measured by UV melting experiments suggest that two guanine bases separated by four AT base pairs constitute the favorable binding site for the PBD dimer. Large stabilizations were observed for the self-complementary duplex $d(AACAATTGTT)_2$ as well as for the non-self-complementary duplex d(AAGAATTGTT)·d(AACAATTCTT) with both guanines located on the same strand. Formation of interstrand and intrastrand crosslinks by the covalent binding of both PBD moieties of the dimer to the exocyclic 2-amino group of the two guanine bases within the duplex minor groove was confirmed by NMR structural studies. In both the symmetric and non-symmetric DNA–PBD adducts the newly created stereogenic center at C11 of the tricyclic PBD subunits favors an *S* configuration. Different orientations of the PBD aromatic A-ring with respect to the covalently modified guanine as observed in the non-symmetric complex are shown to result in characteristic changes of PBD H11 and H11a proton chemical shifts. Based on a compilation of available NMR data on various PBD complexes, these differences may be used as valuable probes for the identification of PBD orientational preferences in DNA–PBD adducts.

Introduction

Pyrrolo[2,1-*c*][1,4]benzodiazepines (PBDs) constitute a family of natural and synthetic compounds with a tricyclic ring system, that have attracted much interest over the last four decades due to their DNA alkylating and cytotoxic activities. Naturally occurring members of the family isolated from various *Streptomyces* species include the anticancer antibiotics anthramycin, tomaymycin and DC-81 (Fig. 1a). It has been shown that PBDs exert their biological activity through binding to duplex DNA, thereby inhibiting vital DNA processing functions like transcription or replication.[1–3] Binding occurs in the DNA minor groove and involves covalent bond formation between the exocyclic amino group of a central guanine within a three base pair recognition site and the electrophilic imine functionality of the diazepine B-ring (Fig. 1b). Likewise, addition products of the imine like carbinolamines or carbinolamine alkylethers may alternatively serve as active PBD species by also triggering guanine adduct formation within the duplex minor groove.

As demonstrated recently, aminal bond formation by nucleophilic attack of the guanine 2-amino group on the PBD C11 electrophilic site constitutes a reversible process.[4] Thus, whereas most of the ligand is cleaved from the DNA following duplex thermal melting at higher temperatures, it can again covalently bind at lower temperatures after re-annealing of complementary strands. Although PBD drugs require double-stranded targets for covalent bond formation, PBD–DNA adducts may nevertheless persist despite DNA strand separation. In fact, single-stranded PBD–DNA adducts of sufficient stability for their isolation and characterization by a combined HPLC/MS methodology have been observed under denaturing solution conditions.[5] Covalent bond formation will also create a new stereogenic center at C11. Whereas only an *S* configuration at the chiral C11a position imparts a twist to the PBD structure that matches the minor groove of a right-handed helix and enables duplex binding, the

[a]*Institute of Biochemistry, Ernst-Moritz-Arndt University Greifswald, Felix-Hausdorff-Str. 4, D-17487 Greifswald, Germany. E-mail: weisz@uni-greifswald.de; Fax: +49 (0)3834 864427; Tel: +49 (0)3834 864426*
[b]*Chemical Biology Laboratory, Division of Organic Chemistry, Indian Institute of Chemical Technology, Hyderabad 500607, India*

†Electronic supplementary information (ESI) available: Molecular model of a crosslinked bis-adduct of **1** and the $d(AACAATTGTT)_2$ duplex; proton chemical shifts and scalar coupling constants of free **1**; proton assignments for the free **A4** duplex as well as for the **S4-1** and **A4-1** complexes; portions of 2D NOE spectra of **A4-1** and **S4-1** complexes. See DOI: 10.1039/c2ob25654a

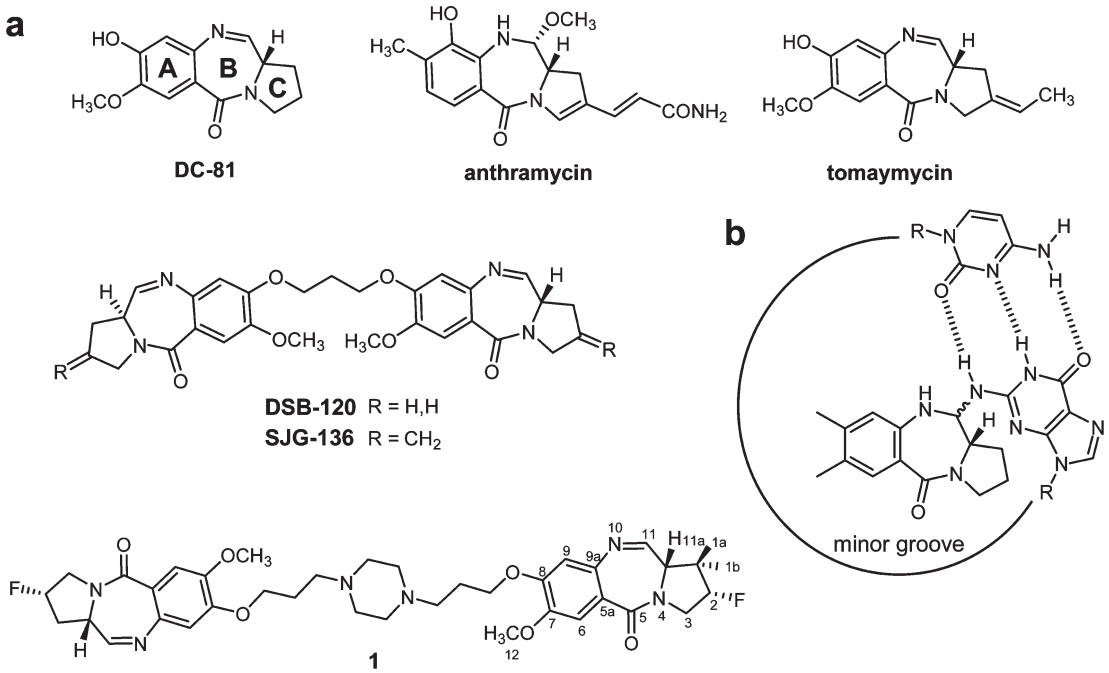

Fig. 1 (a) Structure of DC-81, anthramycin and tomaymycin as well as of the PBD dimers DSB-120, SJG-136 and **1** with atom numbering; (b) pyrrolobenzodiazepine–dG·dC adduct.

configuration at C11 in the formed aminal seems to be less restricted based on structural considerations. However, an 11*S* stereochemistry in guanine adducts is strongly favored over 11*R* stereoisomers as suggested by several theoretical and experimental studies.[6–8] Also, an orientation of the PBD aromatic A-ring towards the 3′-side of the alkylated guanine seems to be preferred, but orientational preferences may strongly depend on DNA sequence and PBD structural features.

Various limitations encountered in the clinical use of the naturally occurring simple PBDs have led to the design and synthesis of a large number of novel and often much more potent PBD drugs in recent years.[9] Conjugates that link the alkylating PBD moiety with other DNA intercalating or minor groove binding motifs have been developed for a better DNA binding affinity.[10,11] Also, synthetic PBD dimers have been of particular interest due to their often significant cytotoxic activity as a result of their crosslinking ability.[12,13] Thus, the C8/C8′ alkane-linked DSB-120 was found to represent a highly efficient DNA crosslinking agent, significantly enhancing the DNA binding ability of its parent compound DC-81.[14] Additional modifications led to the C2/C2′ *exo*-unsaturated analogue SJG-136 with a remarkable *in vitro* and *in vivo* cytotoxic potency. Following phase I clinical trials it is presently undergoing phase II studies based on its promising antineoplastic activity.[15–17]

Presently, much effort is devoted to the design of dimeric PBD analogues with modified substituents and/or linker units to enhance DNA binding affinity and cytotoxicity. In an attempt to evaluate effects exerted by fluorine substitutions, fluorine was incorporated at the 2-position of the parent DSB-120 dimer in earlier studies but failed to result in a noticeable increase of the DNA binding affinity as suggested by melting experiments on calf thymus (CT) DNA.[18] However, a considerably enhanced duplex stabilization was found when increasing the linker length from a trimethylene to a pentamethylene unit, pointing to the importance of the linker subunit not only for the sequence selectivity but also for the binding affinity. More recently, a 2-fluorinated derivative **1** with a 1,4-di-*n*-propyl piperazine linker (Fig. 1a) was synthesized and tested for its biological activity and its binding to calf thymus DNA.[19] The piperazine ring has previously been shown to provide for a favorable binding interaction in minor groove recognition[20] and was expected to improve the bioavailability as well as the binding affinity of the PBD dimer. Indeed, in addition to its promising anticancer activity remarkable enhancements were found for the thermal stability of CT DNA upon binding **1** with its fluoro substitution and piperazine containing linker.[19] Thus, DNA thermal denaturation studies showed that **1** increases T_m by 37 °C as compared to 26 °C for SJG-136 under identical conditions. Also, modeling studies on **1** pointed to AT-rich regions as preferred binding sites for non-covalent drug–DNA interactions.

Because the biological activity of PBDs is thought to be strongly correlated with their duplex binding affinity and their sequence selectivity in DNA recognition, we here report on binding studies of PBD dimer **1** with different double-helical oligonucleotides. Dimer **1** was selected for the present studies based on its high relative binding affinity towards CT DNA within a series of structural analogues as assessed by initial UV melting experiments.[19] Preferred duplex targets are identified and subjected to an NMR structural analysis to gain insight into potential adduct formation, crosslinking capabilities of the drug and the stereochemistry of covalent bond formation. Finally, NMR spectroscopic parameters are introduced as potential probes for an assessment of PBD orientational preferences upon DNA binding.

Results

UV melting studies

To identify preferred duplexes for the PBD dimer **1**, thermal duplex stabilizations ΔT_m through drug binding were determined by UV melting experiments. These can be used as an approximate measure of favorable drug–DNA interactions within complexes and hence for the binding affinity of the drug towards the double-helical target. The duplexes selected differ in their number of AT base pairs between reactive guanines, the latter being located on either the same (A-duplexes) or the opposite strand (S-duplexes). This may allow for intra- or interstrand crosslinks with the PBD dimer in the case of appropriately spaced guanines.

Initially, thermal melting curves were recorded for double-stranded oligonucleotides in the absence of the PBD dimer, exhibiting a single cooperative melting transition. Following the addition of drug in a fourfold excess over the duplex, a biphasic melting profile with a first transition corresponding to the free duplex melting and a second high-temperature transition indicating dissociation of a formed 1 : 1 complex is observed (Fig. 2). Also, as reported before for other PBD adducts with G-containing duplexes,[21] only the low-temperature transition corresponding to the annealing of the free single strands is observed upon a subsequent cooling cycle (not shown). Apparently, the PBD dimer dissociates from the DNA following strand separation at higher temperatures and another DNA adduct is only formed after re-annealing of the two oligonucleotide strands to a duplex at lower temperatures.

All duplexes carrying two reactive guanine bases are considerably stabilized when forming a complex with the PBD dimer with ΔT_m values ranging from 19 °C up to 47 °C (see Table 1). The largest duplex thermal stabilizations with ΔT_m values >40 °C are observed for duplexes **S4**, **S4r** and **A4** with four AT base pairs between guanines, allowing for a potential 1,6-intra- or interstrand crosslink with **1**. A shortened or elongated AT base pair tract between the two guanine binding sites results in a decreased stabilization ΔT_m upon drug binding. There seems to be no general preference for duplexes of the S-series with the two guanines located on opposite strands or the A-series with two guanines on the same strand and amenable to a potential intrastrand crosslink with the PBD dimer. Except for differences in ΔT_m as a result of guanine separation, complex stabilities as expressed in terms of ΔT_m seem to depend on the particular base sequence at the binding sites in a subtle way. Small differences in thermal stabilization are also observed for duplexes **S4** and **S4r** having a reversed strand polarity and expected to result in an opposite drug orientation within the complexes.

As mentioned above, two transitions corresponding to the melting of PBD complexes and the low-temperature melting of a residual free duplex are observed in the UV melting profiles unless solutions are equilibrated for a prolonged period of time (Fig. 2). If the single annealing transition of a free duplex, as is exclusively observed in the UV cooling profiles, is taken as evidence of an almost complete drug dissociation at temperatures $T > T_{m2}$ and using our standard protocol of recording a second heating curve following cooling and a 10 min waiting period, the ratio of hyperchromicities for the first and second transition may be used as an, albeit rough, measure for the population of coexisting species and therefore for the relative kinetics of drug binding. Thus, PBD complex formation slows down among duplexes in the order **S6**/**S5** > **S3** > **S4** > **A4**. Obviously, the kinetics of PBD binding is not correlated with the complex thermal stability in line with recent data, suggesting different rank orders of sequences based on either kinetic or thermodynamic preferences.[22]

Table 1 Duplex melting temperatures T_m (°C) from temperature dependent UV experiments without and with bound **1**[a]

Duplex	Sequence	T_{m1} w/o **1**	T_{m2} with **1**	ΔT_m[b]
S2	5′-AAATCTTGTT-3′ 3′-TTTAGAACAA-5′	25.4 ± 0.6	55.4 ± 0.1	30.0 ± 0.6
A2	5′-AAATGTTGTT-3′ 3′-TTTACAACAA-5′	28.7 ± 0.6	54.4 ± 0.5	25.7 ± 0.8
S3	5′-AAACATTGTT-3′ 3′-TTTGTAACAA-5′	24.3 ± 0.6	55.3 ± 0.6	31.0 ± 0.9
A3	5′-AAAGATTGTT-3′ 3′-TTTCTAACAA-5′	27.8 ± 0.1	67.8 ± 0.4	40.0 ± 0.4
S4	5′-AACAATTGTT-3′ 3′-TTGTTAACAA-5′	30.3 ± 0.6	77.3 ± 0.6	47.0 ± 0.9
S4r	5′-TTGTTAACAA-3′ 3′-AACAATTGTT-5′	21.7 ± 1.5	64.4 ± 0.5	42.7 ± 1.6
A4	5′-AAGAATTGTT-3′ 3′-TTCTTAACAA-5′	28.0 ± 0.1	70.1 ± 0.1	42.1 ± 0.1
S5	5′-AACAAATTGTT-3′ 3′-TTGTTTAACAA-5′	31.7 ± 1.5	60.7 ± 1.1	29.0 ± 1.9
A5	5′-AAGAAATTGTT-3′ 3′-TTCTTTAACTT-5′	32.0 ± 0.2	57.6 ± 1.6	25.6 ± 1.6
S6	5′-AACAAATTTGTT-3′ 3′-TTGTTTAAACAA-5′	38.8 ± 1.5	60.4 ± 0.6	21.6 ± 1.6
A6	5′-AAGAAATTTGTT-3′ 3′-TTCTTTAAACAA-5′	35.7 ± 0.5	59.4 ± 0.6	23.7 ± 0.8
S7	5′-AACAAAATTTGTT-3′ 3′-TTGTTTTAAACAA-5′	40.9 ± 0.6	59.6 ± 0.3	18.7 ± 0.7
S8	5′-AACAAAATTTTGTT-3′ 3′-TTGTTTTAAAACAA-5′	46.0 ± 0.1	67.7 ± 0.6	21.7 ± 0.6

[a] Averaged values with standard deviations from ≥3 independent measurements. [b] Uncertainties in ΔT_m values were calculated based on error propagation upon data subtraction.

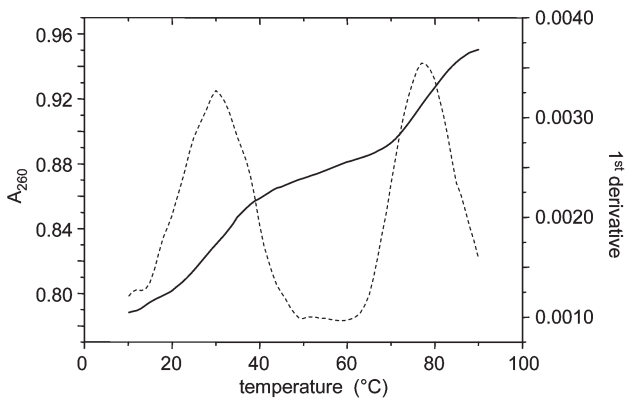

Fig. 2 UV melting curve and its first derivative (broken line) on a mixture of **S4** and **1** (1 : 4 molar ratio).

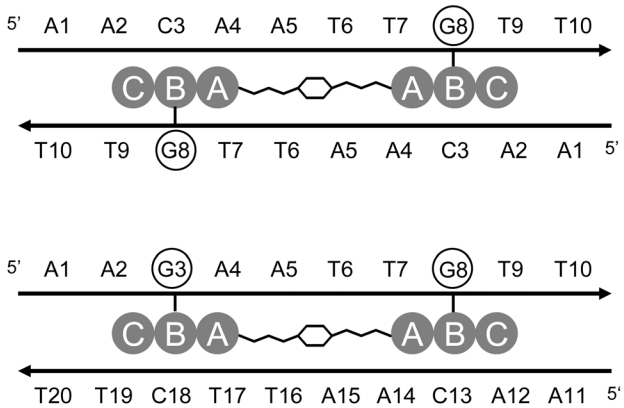

Fig. 3 Duplex **S4** (top) and **A4** (bottom) with nucleotide numbering and a schematic representation of inter- and intramolecular crosslinks by **1**.

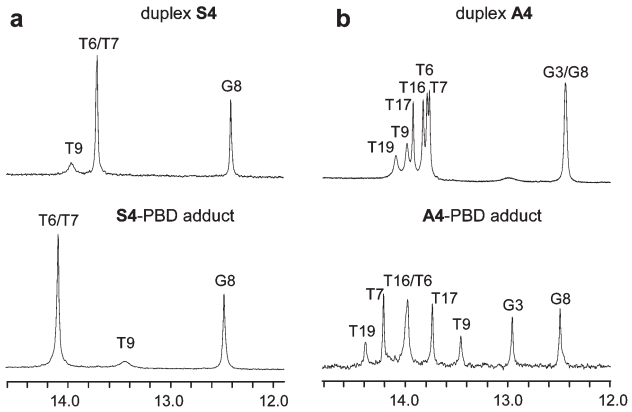

Fig. 4 Imino proton spectral region at 283 K of (a) duplex **S4** and (b) duplex **A4** in the absence of drug (top) and after drug binding (bottom).

NMR structural studies

Consistent with the results from our UV melting experiments, simple molecular models show a four base pair tract between the two guanines to match the geometry of the fluorinated PBD dimer upon potential bis-alkylation. Thus, energy minimizations of a crosslinked model keeping only Watson–Crick hydrogen bonds fixed result in an **S4** bis-adduct with a relaxed piperazine-containing linker, nicely accommodated within the minor groove of a regular non-distorted helix (see ESI Fig. S1†). In the following, the two decamer duplexes **S4** and **A4** were used for additional NMR structural investigations. Potential bis-adducts formed with dimer **1** are shown in Fig. 3.

Whereas resonances of duplex **S4** with its twofold axis of symmetry have been assigned and reported previously,[23] the non-symmetric duplex **A4** was initially subjected to an NMR analysis based on established strategies for oligonucleotide duplexes.[24–26] As with **S4**, the overall pattern of NOE crosspeaks and their relative intensities are consistent with a right-handed double helix, a glycosidic torsion angle in the anti-range and an S-type sugar pucker characteristic of B-DNA.[27]

NMR titration and formation of drug–DNA complexes

Titration of duplex **S4** with the PBD dimer leads to the appearance of new imino proton resonances. Upon saturation with the drug, two resolved sharp and one broadened imino signal due to the penultimate AT base pair are observed (see Fig. 4a). While the terminal imino signal is broadened beyond detection, the downfield shifted signal at 14.10 ppm is associated with two AT imino resonances nearly isochronous under the present experimental conditions as is the resonance at 13.72 ppm seen in the free duplex. It should be mentioned that due to the slow kinetics of adduct formation most of the free duplex has disappeared after one day, but only after a few days the duplex has fully reacted and only imino signals of the PBD–DNA complex remain observable. Because the number of new signals after equilibration equals the number of signals for the free duplex, only one specific PBD–**S4** adduct with the conservation of symmetry must have formed.

For the free non-self-complementary duplex **A4** seven resolved imino proton signals are observed at 283 K (see Fig. 4b). Whereas the two somewhat broadened and most downfield shifted resonances correspond to iminos of the penultimate AT base pairs, the most upfield shifted imino resonance at 12.44 ppm consists of two overlapping iminos of the two GC base pairs. Addition of saturating amounts of **1** ultimately results in significant imino proton chemical shift changes and two separated G imino resonances for the complex below 13 ppm. However, the number of imino resonances does not change after drug binding and again points to the formation of a single well-defined associate (Fig. 4b). Note that imino protons of the terminal base pairs are again unobservable due to fraying effects in both the free duplex and the complex.

As already indicated by the UV melting experiments and corroborated by the time dependent development of imino signals for the complex, the kinetics of the PBD–**A4** complex formation is exceedingly slow. In fact, relative signal intensities in the guanine imino proton spectral region suggest that still about 25% of the free duplex coexist with the complex after 48 h even with a fourfold excess of the added drug. Because both guanine imino protons of the formed complex are spectrally resolved (see Fig. 4), their signals can be easily followed with time. Based on their slow but parallel intensity changes, a faster binding event at a potentially favored guanine site followed by slower binding at the other guanine in **A4** may be excluded (not shown).

DNA proton assignments of the complexes

After completion of complex formation as indicated by the absence of residual signals from the free duplex, DNA resonances of the two complexes were assigned by analyzing 2D NOE, COSY and TOCSY spectra. Overall, the general pattern of NOE intensities suggests a non-distorted B-type duplex for both the **S4** and **A4** complexes. Labile protons were assigned based on imino–imino, imino–amino/H2 as well as amino–amino contacts in NOESY spectra with a 200 ms mixing time acquired in H_2O. Assignments for non-exchangeable DNA protons mostly rely on intranucleotide and sequential base H6/H8 to H1′, H3′, H2′/H2″ and TCH_3 protons. Thus, a network of non-disrupted NOE connectivities along the oligonucleotide strands enables the

straightforward assignment of all H6/H8 and H1′ sugar protons (see ESI Fig. S2†). In addition to H1′ and adenine H2 protons, H4′ protons may also constitute important markers for interactions within the minor groove. However, because an unambiguous assignment was impeded in the strongly overlapped H4′/H5′/H5″ sugar proton spectral region and because we did not seek for a detailed high-resolution structure of the complexes, we refrained from assigning the latter protons.

S4-1 adduct

Following imino proton assignments, a strong crosspeak observed between a proton at 8.38 ppm and the G8 imino proton in the H_2O NOE spectrum identifies a single guanine amino proton typical for a 2-amino alkylation. Another strong crosspeak of the G amino to the newly formed PBD H10 resonance at 7.0 ppm corroborates covalent bond formation with the PBD imine functionality. The G amino and PBD H10 proton share several NOE contacts to the same DNA and drug protons that include **1** H11, **1** H11a as well as A4 H2 and A4 H1′ protons located in the duplex minor groove. A conspicuously strong crosspeak to A4 H2 together with weaker NOE contacts to A5 H2 and PBD H10 in H_2O identifies the aromatic H9 proton within the PBD A-ring and confirms its insertion edge-on into the duplex minor groove with H9 facing the floor of the groove. H11 and H11a resonances of the drug resonating at 4.91 ppm and 5.30 ppm are most conveniently assigned based on their mutual scalar coupling as observed in COSY experiments. Note that in contrast to H11 the H11a proton shows another scalar coupling to an H1 proton of the PBD pyrrolidine ring. By measuring peak-to-peak separations within the DQF-COSY crosspeak patterns a ^3J(H11,H11a) scalar coupling of ~10.5 Hz can be extracted. Due to its large heteronuclear coupling with the geminal fluorine atom of ^2J = 53 Hz, the PBD H2a doublet signal at 5.58 ppm is easily identified in the non-decoupled 2D spectra. Both H2a and H11a exhibit an intermolecular NOE contact to T9 H1′ (see ESI Fig. S3†). A crosspeak between H11 and A4 H1′ is strongly indicated but remains ambiguous due to some signal overlap. Proton assignments for the drug–**S4** adduct are given in the ESI Table S3.†

A4-1 adduct

Covalent bond formation at the two guanines within the same strand is apparent from the presence of two single G amino protons showing a characteristic NOE contact to their G imino proton as well as from the identification of two additional PBD H10 protons resonating at 6.57 and 6.77 ppm. H9 and H9′ protons of the two PBD moieties covalently bound to G3 and G8, respectively, are again unambiguously identified through their strong NOE contact to H2 of A4 (A14) and their additional weaker crosspeak to H2 of A5 (A15). These contacts also clearly indicate the insertion of both PBDs into the duplex minor groove. Other protons of the two non-equivalent PBD moieties of **1** were mostly assigned through their scalar couplings in DQF-COSY and TOCSY spectra. Heteronuclear couplings to the pyrrolidine 2-fluorine substituent of ^3J(H1a,F) ~ 46 Hz, ^3J(H3a, F) ~ 40 Hz and ^2J(H2a,F) ~ 53 Hz strongly facilitated assignment of the pyrrolidine protons in the two PBD moieties of the complex and their identification in the NOESY spectra.

Both pairs of H11 and H11a protons exhibit prominent crosspeaks in DQF-COSY spectra with ^3J(H11,H11a) vicinal couplings of 10.4 Hz and 10.0 Hz as measured from the peak-to-peak separation of antiphase components as shown in Fig. 5. The critical discrimination of H11 and H11a protons is accomplished through their well resolved crosspeak pattern and the observation of another passive ^3J(H11a,H1a) coupling of 7 Hz and 8 Hz. H11a at 3.88 ppm and H11 at 6.0 ppm show NOE contacts to T19 H1′ and A4 H1′ anomeric sugar protons of the duplex, respectively. On the other hand, the additional H11a′ resonance at 5.34 ppm and the H11′ signal at 4.91 ppm exhibit corresponding dipolar couplings to T9 H1′ and A14 H1′ protons (see Fig. 6). These connectivities place the former to the modified G3 nucleotide and identify the latter as part of the G8 alkylating PBD structure. Albeit of lower intensity, NOE contacts also connect H11 with G3 H1′ as well as H11a′ with G8 H1′. Interestingly, weak intra-PBD NOE contacts are observed between H2a and H11 at the G3 adduct and between H2a′ and H11a′ protons at the G8 covalent binding site (see Table 2). This indicates a different puckering of the tricyclic ring system for the two differently oriented PBD subunits and may be compatible with a change from a C2-*endo* towards a C2-*exo* or twisted conformation of the pyrrolidine ring.

Discussion

Based on UV melting data and also indicated by molecular models, the fluorinated PBD dimer **1** with its piperazine-containing linker favors double-helical targets with two central guanines separated by four AT base pairs, irrespective of their positioning on the same or on opposite strands. Recently, experimental and modeling studies on the adduct formation with PBD dimers having $O(CH_2)_3O$ and $O(CH_2)_5O$ linkers demonstrated that these alkane-linked PBDs require target sequences with 2 ± 1 and 3 ± 1 AT base pairs between reacting guanines for efficient crosslinking, respectively.[28] Also, with a larger separation of guanines a preferential formation of intrastrand *versus* interstrand crosslinks was observed. The favorable spacing of only four base pairs between guanines as observed here for the duplex binding of **1** with its relatively long 1,4-di-*n*-propyl piperazine linker indicates that the piperazine moiety may be subject to specific interactions within the minor groove and does not allow a direct extrapolation of sequence selectivity solely based on simple alkane spacers. It should be noted, however, that the kinetics of adduct formation does not parallel thermal stabilities. Also, melting data do not allow for a discrimination of potentially formed monoalkylated and crosslinked bis-adducts.

For the **S4-1** and **A4-1** complexes, NMR spectroscopic studies unequivocally confirm bis-adduct formation associated with inter- and intrastrand crosslinking. Whereas the formation of DNA interstrand crosslinks by PBD dimers has long been recognized as being a major contributor to the significant biological activity of dimeric PBDs, intrastrand crosslinking has only recently come into focus as an alternative mode of PBD dimer interactions with double-helical DNA.[29,30] Interestingly, an intrastrand crosslink formed by the PBD dimer in **A4** confers

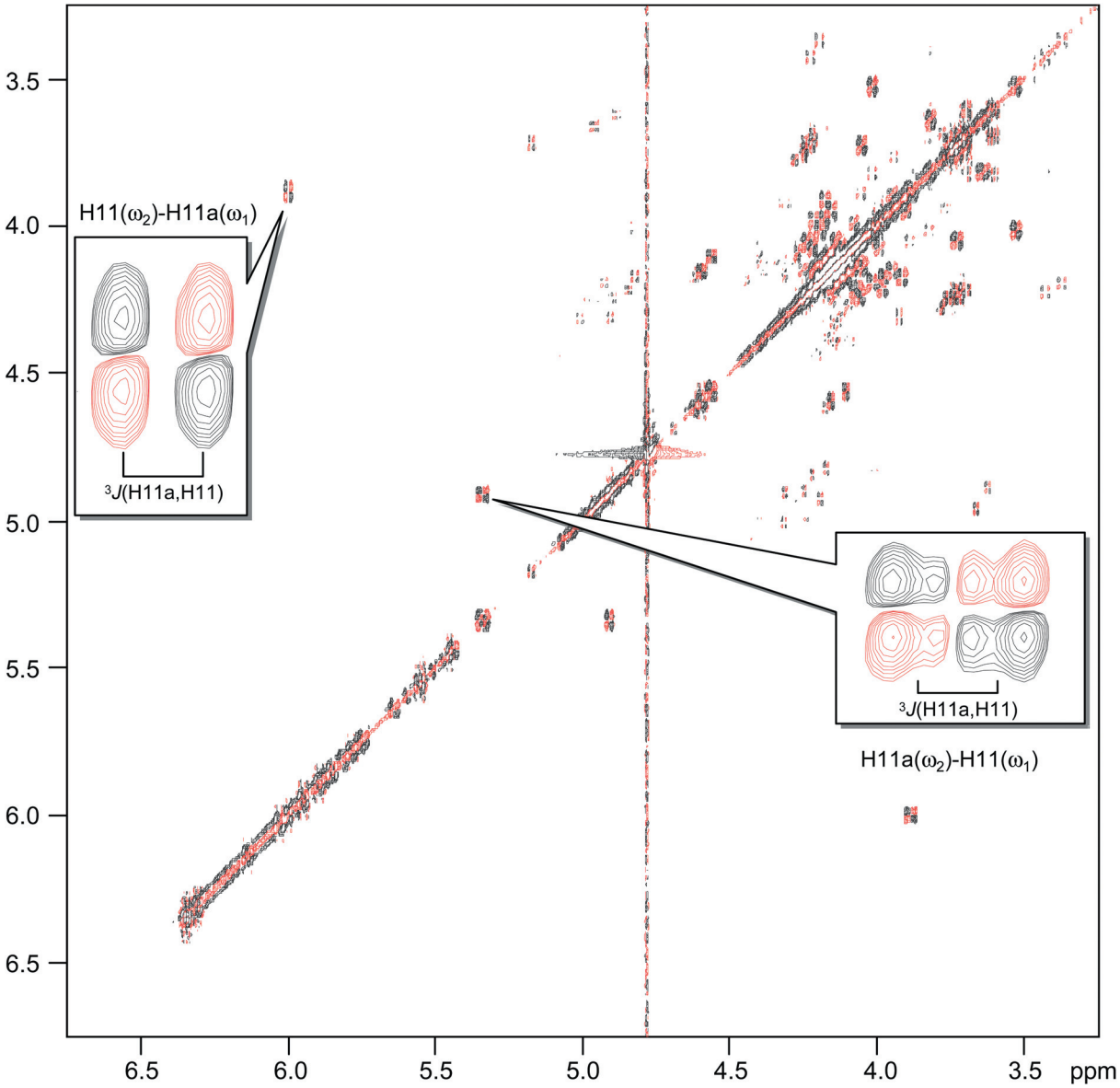

Fig. 5 DQF-COSY spectrum of the **A4-1** adduct acquired at 293 K in D_2O. H11–H11a crosspeaks above the diagonal are enlarged for better discrimination of their different fine structures.

nearly the same thermal stabilization to the duplex as found for the interstrand crosslink in **S4**. Apparently, non-covalent drug–DNA interactions primarily determine the thermal stability of corresponding complexes. On the other hand, if complete strand separation and thus complex denaturation at high temperatures only occurs after drug dissociation, slow hydrolysis of the formed aminal bond between the PBD and guanine may kinetically hamper duplex melting.

Stereochemistry at PBD C11 upon adduct formation

Through the formation of a covalent bond between the pyrrolobenzodiazepine imine function and the 2-amino group of the guanine base, another stereogenic center at C11 of the drug is generated. Starting with an *S*-configuration at C11a, a prerequisite for the accommodation of PBD drugs within the DNA minor groove, two diastereomers (11*S*,11a*S*) and (11*R*,11a*S*) may have formed in a PBD–DNA adduct. In geometry-optimized structures of PBD–9-methylguanine adducts calculated at the B3LYP/6-31+G** level, dihedral angles between H11 and H11a protons are found to be 167° and 75° for the (11*S*,11a*S*) and the (11*R*,11a*S*) diastereomer, respectively. Also, due to their *trans*-disposition in the former configuration, H11a and H11 protons are situated above and below the PBD ring system in close proximity (<4 Å) to H1′ sugar protons on opposite strands. This situation contrasts with corresponding *cis*-oriented PBD H11 and H11a protons of a potential (11*R*,11a*S*) diastereomer and their close proximity to the same H1′ sugar proton on one of the strands (see Fig. 7).

According to the general Karplus relationship, measurements of the vicinal ^3J(H11,H11a) coupling constant in PBD–DNA

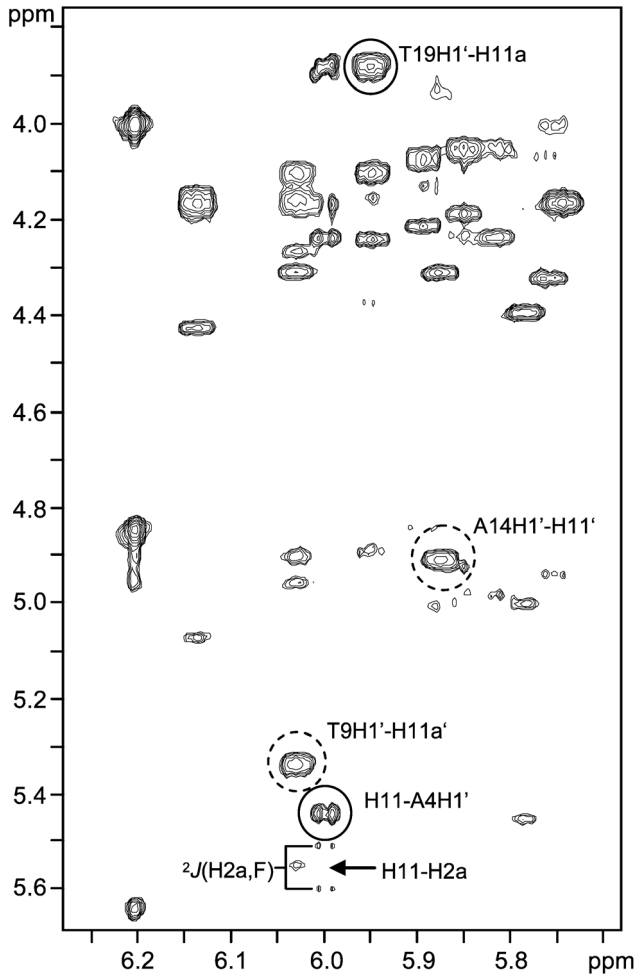

Fig. 6 Portion of a 2D NOE spectrum of the **A4-1** adduct acquired at 293 K in D_2O (120 ms mixing time). Crosspeaks between PBD H11/H11a and DNA H1′ protons are encircled.

Table 2 Experimentally observed NOE contacts of H11/H11a and H11′/H11a′ protons of the two PBD moieties in **1** covalently bound to G3 and G8 of the duplex **A4**, respectively[a]

	H2a/H2a′	A4/T9H1′	A14/T19H1′	G3/G8H1′
H11a	—	—	+++	—
H11	+	+++	—	++
H11a′	+	+++	—	++
H11′	—	—	+++	—

[a] Observed in a 2D NOE spectrum acquired at 293 K in D_2O with a 120 ms mixing time; +, ++ and +++ represent weak, moderate and strong crosspeaks.

adducts should easily discriminate between the two diastereomers. However, unambiguous identification of the C11 configuration may be severely hampered by significant errors in the coupling constant determination if based on simple peak-to-peak separations in COSY crosspeaks with their anti-phase and in-phase patterns and associated with severe amalgamation and cancellation effects in the case of larger signal linewidths. Also, the flexible pyrrolodiazepine ring system will enable the drug to accommodate within the duplex minor groove changing conformational preferences upon binding. In fact, molecular mechanics calculations performed on (11*R*,11a*S*) and (11*S*,11a*S*) DNA–PBD models with the MMFF force field together with torsion angles extracted from published NMR-derived complex structures[23,31,32] point to torsion angles between PBD H11 and H11a protons as low as 142° and 29° for (11*S*,11a*S*) and (11*R*,11a*S*) adducts, respectively. Consequently, whereas a ^3J(H11,H11a) of ≥10 Hz should unambiguously identify an (11*S*,11a*S*) isomeric species, the presence of a corresponding COSY crosspeak as a result of larger coupling does not necessarily exclude the existence of an (11*R*,11a*S*) adduct. On the other hand, an (11*R*,11a*S*) configuration of the PBD drug upon DNA covalent binding is expected to be significantly disfavored according to calculations as well as to experimental evidence. Thus, molecular mechanics and molecular dynamics simulations have shown a clear preference of the 11*S* over the 11*R* configuration of pyrrolobenzodiazepine adducts irrespective of the sequence around the guanine binding site.[6,33,34] To the best of our knowledge there is only one exception to the exclusive finding of (11*S*,11a*S*) configurations determined by NMR in DNA adducts of various PBD drugs. These deviating results were obtained by a combination of NMR, fluorescence and molecular modeling studies and suggested an (11*R*,11a*S*) configuration in addition to a second coexisting (11*S*,11a*S*) species of tomaymycin when bound to calf thymus DNA and to the hexamer duplex $d(ATGCAT)_2$.[35] However, the data did not allow unambiguous identification of diastereoisomers and the tentative assignment of the complexes may be considered disputable.

Based on the above and having determined ^3J vicinal scalar couplings between PBD H11 and H11a protons of 10.5 Hz in **S4-1** as well as of 10.4 Hz and 10.0 Hz for the bis-adduct in **A4**, a C11*S* linkage is clearly indicated for all PBD adducts in the two complexes. This stereochemical assignment is additionally confirmed by corresponding NOESY crosspeaks of H11 and H11a protons. As shown in Fig. 7, H11a and H11 protons are always *trans*-positioned in an 11*S* stereochemical configuration and situated above and below the PBD ring system facing H1′ sugar protons located on opposite strands (*vide infra*). Experimentally observed H11/H11a–H1′ NOE contacts (*e.g.* see Fig. 6) provide evidence for corresponding interproton distances <5 Å in the PBD adducts and are again only compatible with an (11*S*,11a*S*) configuration in all cases.

Orientation of pyrrolobenzodiazepines in DNA adducts

In addition to the potential formation of different configurations at the stereogenic center at C11, the PBD drugs may position themselves within the duplex minor groove with their aromatic A-ring oriented towards the 3′-end of the modified G-strand (3′-orientation) or alternatively towards the 5′-end (5′-orientation). Excluding C11*R*-isomeric species, NMR structural studies in many cases point to a preference for the 3′-orientation in (11*S*,11a*S*) PBD adducts.[36–38] Molecular mechanics simulations also suggest a 3′-orientation favored over a 5′-orientation in complexes with anthramycin and tomaymycin,[6,33] yet opposite preferences were reported for DC-81 in modeling studies involving molecular dynamics simulations.[34] Using hairpin-forming

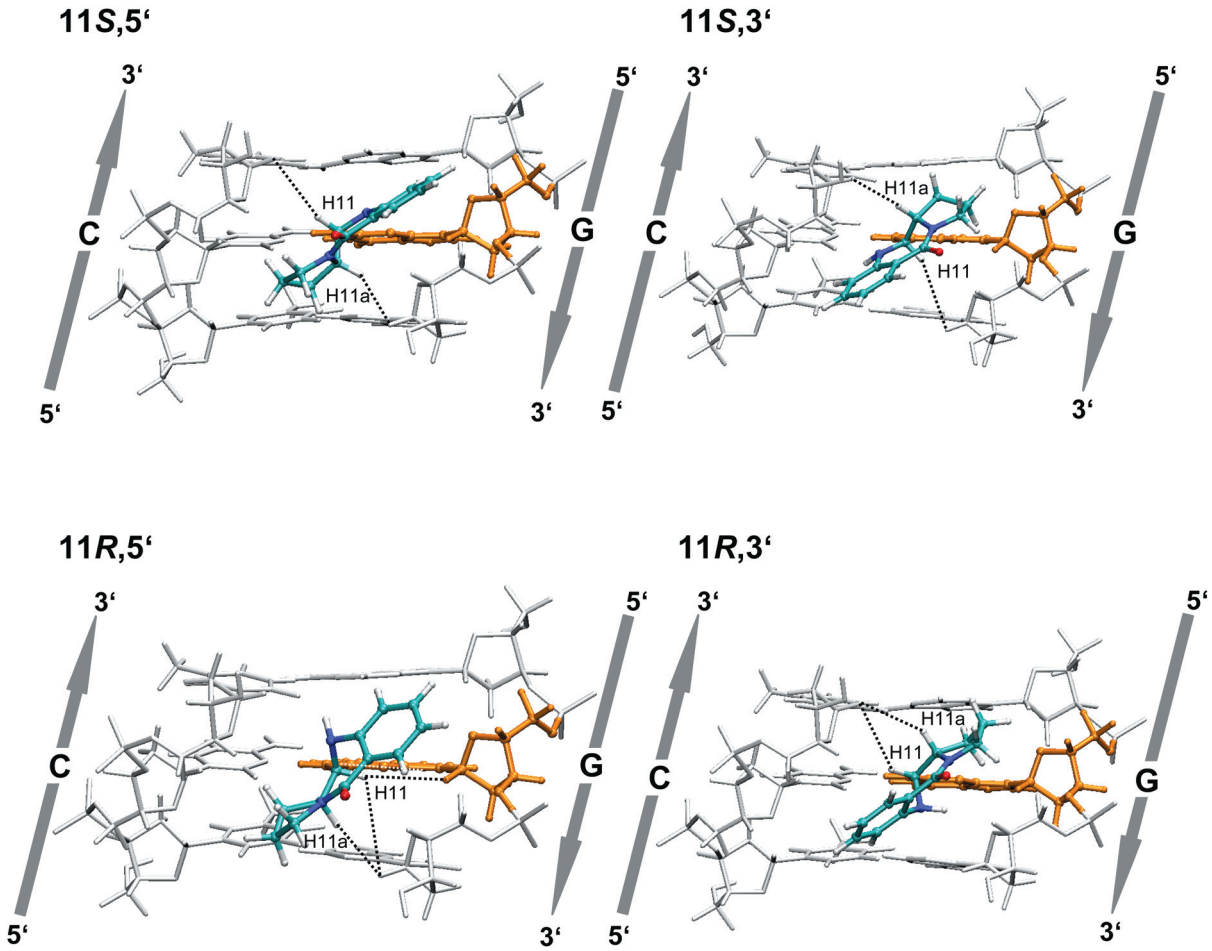

Fig. 7 Views into the minor groove of PBD–DNA adducts with C11*S* (top) and C11*R* (bottom) configurations and a 5′- (left) and 3′-orientation (right); short distances involving PBD H11/H11a and DNA H1′ protons are indicated; covalently modified guanines are highlighted in orange and the tricyclic PBD is shown in atom colors.

oligonucleotides with a single PBD binding site either positioned at the 5′-terminus of the stem region or close to the central loop, a kinetic preference for a 3′-oriented adduct was indicated through HPLC/MS methodologies, yet corresponding 5′-adducts could also form with high reaction rates.[22] Apparently, a 5′-orientation can easily be enforced as has also been shown in complexes of C8-modified PBD hybrids and duplexes carrying a guanine base close to their 3′-terminus.[23,32] It seems that differences in interaction energies are rather small and allow the formation of both types of adducts depending on the particular PBD structure and the sequence of the DNA target. As shown in Fig. 7, an 11*S*,5′ binding mode will place the PBD H11 proton close to the anomeric H1′ sugar proton of the nucleotide at the 3′-side of the cytosine base-paired with the alkylated guanine (*i.e.* nucleotide C + 1). Likewise, H11a will be in close proximity to H1′ of the nucleotide at the 3′-side of the modified guanine (*i.e.* nucleotide G + 1). In contrast, spatial relationships are reversed for an 11*S*,3′ binding mode and thus should allow observation of NOE connectivities between H11 and (G + 1) H1′ as well as between H11a and (C + 1) H1′.

Clearly, in the case of the PBD dimers the orientation of each PBD moiety will necessarily be predetermined when cross-linking the corresponding target duplex (see Fig. 3). Thus, unambiguous NOE contacts place H11a close to T9 H1′ in the **S4-1** adduct as predicted from its 5′-orientation. On the other hand, two different NOE patterns are observed for the **A4-1** complex with its two non-identical PBD moieties oriented in the 3′- and 5′-directions. Here, H11a and H11a′ show NOE contacts to T19 H1′ and T9 H1′ whereas H11 and H11′ protons exhibit dipolar couplings to A4 H1′ and A14 H1′ protons, respectively (Fig. 6).

Although these NOE contacts are reliable diagnostic markers for the PBD orientation, their use requires a prior assignment of drug and DNA resonances. While working on benzimidazole– and naphthalimide–PBD hybrids forming DNA adducts with a 5′-orientation, we noticed considerable changes in the PBD H11 and H11a chemical shifts when compared to published data on PBD adducts with a 3′ drug orientation. Specifically, significant upfield shifts of the H11 resonance in 11*S*,5′ adducts were accompanied by downfield shifts of H11a. These changes resulted in more downfield shifted H11a *versus* H11 protons in contrast to significantly more shielded H11a protons in 11*S*,3′ adducts. Prompted by these initial observations, we compiled available NMR data on 16 PBD–DNA adducts that comprise various PBD drugs bound in different orientations and also include the results on the **1** complexes presented here. In all

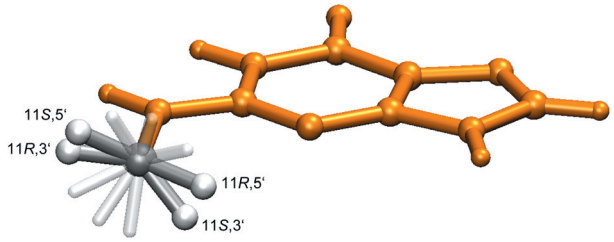

Fig. 8 Molecular model of an amino-alkylated guanine highlighting the location of the PBD H11 proton with respect to the nucleobase for various PBD configurations.

cases, a reversal of H11/H11a relative chemical shifts was observed upon changing drug orientation. Mostly uninfluenced by specific ring puckering modes, the deshielded H11 proton in 11*S*,3′ adducts may be rationalized by its orientation towards the covalently modified guanine and its location within the deshielding region of the purine base. In contrast, the H11 proton in 11*S*,5′ adducts always points away from the guanine ring system and is expected to only experience vanishing ring current effects (Fig. 8).

PBD H11 proton chemical shifts are found to cluster within a relatively narrow range of 4.5 ppm $\leq \delta \leq$ 4.9 ppm for 11*S*,5′ adducts and 5.5 ppm $\leq \delta \leq$ 6.1 ppm for 11*S*,3′ adducts. For PBD H11a protons, observed chemical shifts cover a somewhat wider range from 4.7 ppm to 5.4 ppm in 11*S*,5′ adducts and from 3.8 ppm to 4.5 ppm in 11*S*,3′ adducts. Clearly, the strongly orientation dependent H11 and H11a chemical shift should represent a good marker for the PBD binding, provided that the two PBD proton resonances have been unambiguously assigned. On the other hand, the observation of a chemical shift <4.5 ppm or >5.5 ppm for either proton should reliably identify an 11*S*,3′ adduct under normal experimental conditions even without the need of prior assignments.

In Fig. 9 chemical shifts found for H11 and H11a protons in the various PBD adducts have been correlated in a two-dimensional plot. For PBD 5′-orientations all H11/H11a chemical shift differences are below 1 ppm with corresponding correlations, as for example observable as crosspeaks in a COSY experiment, lying close to the diagonal. In contrast, for PBD 3′-orientations all H11/H11a chemical shift differences are >1 ppm and thus correlations are shifted away from the diagonal. Because the region of H11–H11a crosspeaks in a COSY spectrum is mostly free of additional DNA proton correlation peaks (see Fig. 5), examination of this spectral region can provide for a simple method of identifying the PBD orientation without the need for more extensive proton assignments. Note that the data used for the plot in Fig. 9 not only include different DNA target sequences and slightly different experimental conditions like temperature, but also various PBD derivatives with different substituents as well as C2-*exo* and C2–C3-*endo* unsaturation, giving confidence in their more general validity.

Conclusions

2-Fluoro-substituted pyrrolo[2,1-*c*][1,4]benzodiazepines linked through a 1,4-di-*n*-propyl piperazine linker form 1,6-interstrand

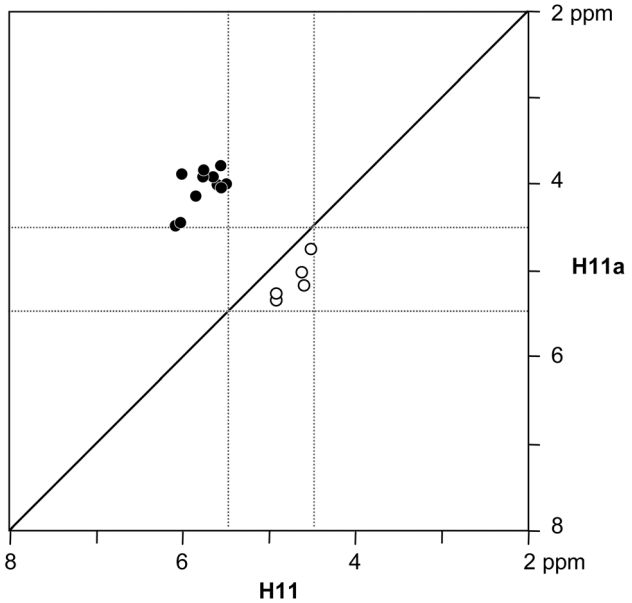

Fig. 9 Chemical shifts of PBD H11 and H11a protons in DNA adducts with 11*S*,5′ (open circles) and 11*S*,3′ binding (closed circles). Data were taken from this study and from ref. 7, 23, 30–32, 36, 37, and 39–41.

as well as intrastrand crosslinks with target duplexes having reactive guanines at appropriate positions. The thermal stability of these bis-adducts is remarkable and suggests strong DNA–drug interactions within the complexes, albeit with relatively slow kinetics of binding. More detailed information on the sequence-dependence of complex stability on the one hand and the kinetics of complex formation on the other hand will be necessary in the future for a better assessment of *in vivo* activities for this type of PBD dimer. In addition, NMR structural studies provide for the stereochemistry at the covalent binding site and for the orientation of the PBD in a given target duplex. In view of an increasing number of PBD-based drugs and the importance of PBD orientational preferences for their sequence selectivity and their mechanism of action, a more rapid and convenient NMR-based assay for the discrimination of PBD binding modes is highly desirable. The stereochemical and orientational dependence of individual PBD proton chemical shifts as presented here may be valuable as an easily accessible marker for PBD geometries in such complexes.

Experimental section

Sample preparation

Duplexes were purchased from *TIB MOLBIOL* (Berlin, Germany) and dissolved in PBS buffer (100 mM NaCl, 20 mM phosphate, pH 7.0) for the UV measurements or in 100 mM NaCl, 1 mM NaN_3, pH 7.0, for the NMR experiments. The drug–DNA complex for the NMR structural studies was prepared by titrating a 0.5 mL solution of the DNA duplex with a concentrated drug solution in DMSO-d_6 up to a 4 : 1 drug-to-duplex molar ratio. The mixture was left at 4 °C until all of the duplex was saturated with drug as evidenced by one-dimensional NMR spectra. Despite being used in excess no resonances of the

PBD dimer could be observed in subsequent NMR experiments due to its poor solubility in the aqueous solution. For some NOESY, TOCSY and DQF-COSY experiments on non-exchangeable protons, NMR samples in 90% H_2O–10% ^2H_2O were lyophilized three times and finally redissolved in 99.996% D_2O. The samples for the NMR studies were about 1 mM in a duplex.

UV melting experiments

UV thermal denaturation studies were performed in 1 cm quartz cuvettes on the duplexes in the absence or presence of the PBD dimer. The duplex concentration was 3.5 μM for all experiments. For the mixtures, a DMSO solution of the PBD was added to an equilibrated solution of the duplex in a 1 : 4 duplex-to-drug molar ratio 1 h prior to the measurements. The final DMSO content of the solutions was less than 1.5%. The melting curves were recorded with a *Cary 100* spectrophotometer equipped with a Peltier temperature control unit (*Varian* Deutschland, Darmstadt) by measuring the absorbance of the solution at 260 nm as a function of temperature. A protocol was applied, that was initiated by first heating from 10 °C to 90 °C followed by cooling the sample to the starting temperature. After a waiting period of 10 min another heating ramp was started. Heating rates of 0.5 °C min^{-1} were employed. In general, melting temperatures were determined by the maximum of the first derivative plot of the second heating curves and are given as averages from at least three independent experiments. For some duplex–drug mixtures, measurements were repeated after incubation for 1 day at room temperature but did not result in changes of determined transition temperatures.

NMR experiments

^1H NMR experiments were performed on a Bruker Avance 600 MHz spectrometer equipped with an inverse $^1H/^{13}C/^{15}N/^{31}P$ quadruple resonance cryoprobehead and *z*-field gradients. A combination of phase-sensitive nuclear Overhauser effect spectroscopy (120 and 200 ms mixing time NOESY) as well as through bond correlated (COSY, phase-sensitive DQF-COSY) and total correlated spectroscopy (80 and 120 ms spin-lock time TOCSY with a DIPSI2 or MLEV17 spin-lock and a field strength of 7.1 kHz) was applied for the samples in the States-TPPI mode except for magnitude mode COSY experiments. Typically, for assignments of non-exchangeable protons 2D spectra in D_2O were acquired at 293 K with a sweep width of 6600 Hz and the carrier frequency set to the HDO resonance frequency. Residual HDO was suppressed with a 3–9–19 WATERGATE sequence or by presaturation during the relaxation delay as required. A total of 1024 FIDs of 4096 complex data points were collected in t_1 with 32 transients at each t_1 value and a recycle delay of 2 s. Prior to Fourier transformation, the FIDs were zero-filled to give a 4K × 4K or 4K × 2K data set. Both dimensions were apodized with phase-shifted sine or squared sinebell functions. Proton chemical shifts were referenced to the HDO peak taking into account the temperature dependence of its chemical shift.

For the assignments of exchangeable protons, 2D NOE experiments in 90% H_2O–10% ^2H_2O were acquired at 283 K with a 200 ms mixing time and a spectral width of 14 000 Hz using either the DPFGSE or the 3–9–19 WATERGATE pulse sequence for solvent suppression. Corresponding suppression schemes were also used for 1D experiments in H_2O.

Molecular modeling

Model building, molecular mechanics and *ab initio* calculations were performed using Spartan'08 (Wavefunction Inc., Irvine, CA, USA). Crosslinked bis-adducts were built by covalent bond formation between guanine N2 and C11 with an *S*-configuration of each PBD subunit in the duplex minor groove. The two covalently attached PBD moieties were subsequently connected by the dialkyl piperazine linker and the complex minimized in two steps. In step 1 all atoms of the DNA duplex were fixed to only allow relaxation of the PBD dimer. In a second step all atoms were released but Watson–Crick hydrogen bonds were still constrained to prevent unstacking of bases in the minimization procedure without additional solvent and counterions.

References

1 L. H. Hurley and R. L. Petrusek, *Nature*, 1979, **282**, 529–531.
2 R. L. Petrusek, G. L. Anderson, T. F. Garner, Q. L. Fannin, D. J. Kaplan, S. G. Zimmer and L. H. Hurley, *Biochemistry*, 1981, **20**, 1111–1119.
3 L. H. Hurley, T. Reck, D. E. Thurston, D. R. Langley, K. G. Holden, R. P. Hertzberg, J. R. E. Hoover, G. Gallagher, L. F. Faucette, S. M. Mong and R. K. Johnson, *Chem. Res. Toxicol.*, 1988, **1**, 258–268.
4 K. M. Rahman, C. H. James and D. E. Thurston, *Org. Biomol. Chem.*, 2011, **9**, 1632–1641.
5 K. M. Rahman, C. H. James, T. T. T. Bui, A. F. Drake and D. E. Thurston, *J. Am. Chem. Soc.*, 2011, **133**, 19376–19385.
6 S. N. Rao, U. C. Singh and P. A. Kollman, *J. Med. Chem.*, 1986, **29**, 2484–2492.
7 T. R. Krugh, D. E. Graves and M. P. Stone, *Biochemistry*, 1989, **28**, 9988–9994.
8 M. L. Kopka, D. S. Goodsell, I. Baikalov, K. Grzeskowiak, D. Cascio and R. E. Dickerson, *Biochemistry*, 1994, **33**, 13593–13610.
9 A. Kamal, M. V. Rao, N. Laxman, G. Ramesh and G. S. K. Reddy, *Curr. Med. Chem.: Anti-Cancer Agents*, 2002, **2**, 215–254.
10 A. Kamal, R. Ramu, V. Tekumalla, G. B. R. Khanna, M. S. Barkume, A. S. Juvekar and S. M. Zingde, *Bioorg. Med. Chem.*, 2008, **16**, 7218–7224.
11 A. Kamal, P. Ramulu, O. Srinivas, G. Ramesh and P. P. Kumar, *Bioorg. Med. Chem. Lett.*, 2004, **14**, 4791–4794.
12 S. J. Gregson, P. W. Howard, D. R. Gullick, A. Hamaguchi, K. E. Corcoran, N. A. Brooks, J. A. Hartley, T. C. Jenkins, S. Patel, M. J. Guille and D. E. Thurston, *J. Med. Chem.*, 2004, **47**, 1161–1174.
13 S. J. Gregson, P. W. Howard, J. A. Hartley, N. A. Brooks, L. J. Adams, T. C. Jenkins, L. R. Kelland and D. E. Thurston, *J. Med. Chem.*, 2001, **44**, 737–748.
14 D. S. Bose, A. S. Thompson, J. Ching, J. A. Hartley, M. D. Berardini, T. C. Jenkins, S. Neidle, L. H. Hurley and D. E. Thurston, *J. Am. Chem. Soc.*, 1992, **114**, 4939–4941.
15 S. J. Gregson, P. W. Howard, T. C. Jenkins, L. R. Kelland and D. E. Thurston, *Chem. Commun.*, 1999, 797–798.
16 M. Narayanaswamy, W. J. Griffiths, P. W. Howard and D. E. Thurston, *Anal. Biochem.*, 2008, **374**, 173–181.
17 Y. Y. Janjigian, W. Lee, M. G. Kris, V. A. Miller, L. M. Krug, C. G. Azzoli, E. Senturk, M. W. Calcutt and N. A. Rizvi, *Cancer Chemother. Pharmacol.*, 2010, **65**, 833–838.
18 A. Kamal, P. S. M. M. Reddy and D. R. Reddy, *Bioorg. Med. Chem. Lett.*, 2004, **14**, 2669–2672.
19 A. Kamal, D. Rajender, D. R. Reddy, M. K. Reddy, G. Balakishan, T. B. Shaik, M. Chourasia and G. N. Sastry, *Bioorg. Med. Chem.*, 2009, **17**, 1557–1572.

20 C. E. Bostock-Smith and M. S. Searle, *Nucleic Acids Res.*, 1999, **27**, 1619–1624.
21 M. Rettig, A. Kamal, R. Ramu, J. Mikolajczak and K. Weisz, *Bioorg. Med. Chem.*, 2009, **17**, 919–928.
22 M. Rahman, H. Vassoler, C. H. James and D. E. Thurston, *ACS Med. Chem. Lett.*, 2010, **1**, 427–432.
23 M. Rettig, M. Weingarth, W. Langel, A. Kamal, P. P. Kumar and K. Weisz, *Biochemistry*, 2009, **48**, 12223–12232.
24 J. Feigon, J. M. Wright, W. Leupin, W. A. Denny and D. R. Kearns, *J. Am. Chem. Soc.*, 1982, **104**, 5540–5541.
25 R. M. Scheek, N. Russo, R. Boelens, R. Kaptein and J. H. van Boom, *J. Am. Chem. Soc.*, 1983, **105**, 2914–2916.
26 P. Rajagopal, D. E. Gilbert, G. A. van der Marel, J. H. van Boom and J. Feigon, *J. Magn. Res.*, 1988, **78**, 526–537.
27 K. Wüthrich, *NMR of Proteins and Nucleic Acids*, John Wiley & Sons, New York, 1986.
28 K. M. Rahman, C. H. James and D. E. Thurston, *Nucleic Acids Res.*, 2011, **39**, 5800–5812.
29 K. M. Rahman, A. S. Thompson, C. H. James, M. Narayanaswamy and D. E. Thurston, *J. Am. Chem. Soc.*, 2009, **131**, 13756–13766.
30 S. R. Hopton and A. S. Thompson, *Biochemistry*, 2011, **50**, 4720–4732.
31 D. Antonow, T. Barata, T. C. Jenkins, G. N. Parkinson, P. W. Howard, D. E. Thurston and M. Zloh, *Biochemistry*, 2008, **47**, 11818–11829.
32 M. Rettig, W. Langel, A. Kamal and K. Weisz, *Org. Biomol. Chem.*, 2010, **8**, 3179–3187.
33 W. A. Remers, M. Mabilia and A. J. Hopfinger, *J. Med. Chem.*, 1986, **29**, 2492–2503.
34 L. J. Adams, T. C. Jenkins, L. Banting and D. E. Thurston, *Pharm. Pharmacol. Commun.*, 1999, **5**, 555–560.
35 M. D. Barkley, S. Cheatham, D. E. Thurston and L. H. Hurley, *Biochemistry*, 1986, **25**, 3021–3031.
36 J. A. Mountzouris, J.-J. Wang, D. Thurston and L. H. Hurley, *J. Med. Chem.*, 1994, **37**, 3132–3140.
37 F. L. Boyd, S. F. Cheatham, W. Remers, G. C. Hill and L. H. Hurley, *J. Am. Chem. Soc.*, 1990, **112**, 3279–3289.
38 T. C. Jenkins, L. H. Hurley, S. Neidle and D. E. Thurston, *J. Med. Chem.*, 1994, **37**, 4529–4537.
39 S. Cheatham, A. Kook, L. H. Hurley, M. D. Barkley and W. Remers, *J. Med. Chem.*, 1988, **31**, 583–590.
40 F. L. Boyd, D. Stewart, W. A. Remers, M. D. Barkley and L. H. Hurley, *Biochemistry*, 1990, **29**, 2387–2403.
41 J.-J. Wang, G. C. Hill and L. H. Hurley, *J. Med. Chem.*, 1992, **35**, 2995–3002.

